NITROXIDES AND MALIGNANT HUMAN TISSUES: ELECTRON SPIN RESONANCE IN COLORECTAL NEOPLASTIC AND HEALTHY TISSUES.

ELSEVIER

Biochimica et Biophysica Acta 1472 (1999) 1–12

BIOCHIMICA ET BIOPHYSICA ACTA
BBA

www.elsevier.com/locate/bba

Nitroxides and malignant human tissues: electron spin resonance in colorectal neoplastic and healthy tissues

Simona Rossi [a], Annalisa Giuntini [a], Manuela Balzi [b], Aldo Becciolini [b], Giacomo Martini [a,*]

[a] *Dipartimento di Chimica, Università di Firenze, Via G. Capponi 9, 50121 Firenze, Italy*
[b] *Laboratorio di Radiobiologia, Dipartimento di Fisiopatologia Clinica, Università di Firenze, Viale Pieraccini 6, 50134 Firenze, Italy*

Received 17 February 1999; received in revised form 10 May 1999; accepted 2 June 1999

Abstract

Healthy and neoplastic colorectal human tissues of as many as 12 patients have been studied, immediately after surgery, by electron spin resonance (ESR) of stable nitroxides at physiological temperature. Cells were maintained in a living state using the McCoy's 5A culture medium. The very low concentration changes of hydrophilic and lipophilic nitroxides allowed us to establish that the response to the oxidative stress induced by the occurrence of nitroxides in healthy and tumor cells was very weak, thus suggesting these compounds are good candidates for contrast enhancement agents in magnetic resonance imaging of colorectal tumor. The analysis of the computed ESR line shape of lipophilic nitroxides in both healthy and malignant cells of the same patient agreed for an unmodified physical status of the membranes where they were mainly localized. The results reported here proved that the comparison between ESR results must be made in tissues from the same patient and that the physical status of the membranes depended more on the patient history than on changes in the colorectal cell membrane fluidity induced by the neoplastic process.

Keywords: Electron spin resonance; Human colorectal cancer; Membrane fluidity; Nitroxide reduction; Spin probe

1. Introduction

In western countries, malignant neoplastic diseases are the second human death cause, after heart diseases. The factors affecting the cancer development are various, including the individual genetic constitution, the environmental status and the personal life style. During the last phase in the altered cell proliferation, the so-called 'progression', qualitative cell changes appear, which are inherited and irreversible. All information at a molecular level on these aspects is therefore of help to give light on the mechanisms of alteration of cell proliferation.

Magnetic resonance spectroscopies are certainly the most promising tools to obtain resolution at the molecular level on cancer diseases. A large part of the work carried out till now involves nuclear magnetic resonance (NMR) at its various levels of sophistication, including magnetic resonance imaging (MRI), which is now routine technique in the clinical diagnosis of neoplasias [1].

Experiments have also been carried out by electron spin resonance (ESR) of radicals formed during the process in tumoral tissues. The direct observation of radicals supposed to be generated by cancer develop-

* Corresponding author. Fax: +39-55-244102;
E-mail: martini@cf.chim.unifi.it

0304-4165/99/$ – see front matter
PII: S0304-4165(99)00092-6

ment is limited to very weak, unresolved signals whose interpretation is not straightforward [2–7]. Spin traps have also been used in some cases [8–11]. Nitroxides, as externally added stable paramagnetic radicals, have given more reliable results, and have been applied by many researchers [12–18]. The most used nitroxides contain a wide variety of functional groups; they are easily synthesized, may be covalently attached to biomacromolecules, and usually have a long half-life and a relatively high stability at physiological pH and temperature.

Nitroxides can also protect normal tissues from oxidative (SOD-like activity) and radiation damage [19–24] and have been considered as attractive contrast enhancing agents in MRI because of their effect on T_1 and T_2 of the biological fluid protons [25–29]. Swartz [30] suggests the use of nitroxides as metabolically responsive contrast agents because of their metabolism dependence on oxygen. The concept of a substance that can be used to control the relative intensities of different regions of a magnetic resonance image was first recognized by Lauterbur et al. [31] and proved by previously documented effect of paramagnetic metal ions (mainly Gd(III) and Mn(II) complexes) on nuclear relaxation times of many nuclides, especially ^{1}H and ^{13}C [32]. Recently, classes of paramagnetic compounds other than Gd-DTPA [33] have been invented which can similarly alter image contrast in vivo; these include those based on stable nitroxide radicals [34].

Nitroxide probes are in fact readily incorporated into living cells. Because of the different structure, size and properties of the nitroxides used in living beings, their metabolism and toxicity are not completely understood at the moment, either in laboratory animals or in man. This is a serious obstacle hampering a wide application of these compounds to MRI [35,36]. The tendency of nitroxides to be biologically reduced through a one-electron mechanism, possibly to the corresponding diamagnetic hydroxylamines, is well documented [29,37–50], although the toxicity of these reduced products has never been investigated thoroughly. Lung, liver, and kidney were found to be the primary sites of in vivo nitroxide reduction in rat [40] and in guinea pig [51]. This has pushed the research toward the design of new, reduction resistant nitroxide-based MRI contrast agents [52–55].

In this study, we used commercially available small and large nitroxides to clarify the effect of neoplastic processes on the colon cell membrane dynamic. Furthermore, their oxidizing properties towards weak reductants, when added in a small concentration to suspensions of colorectal neoplastic and healthy living human cells immediately after surgery were investigated.

2. Materials and methods

2.1. Paramagnetic probes

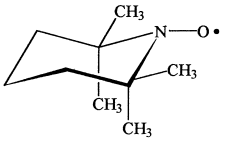

2,2,6,6-tetramethylpiperidine-1oxyl (TEMPO)

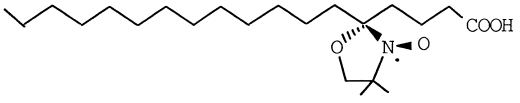

5-doxyl stearic acid (5-DXSA)

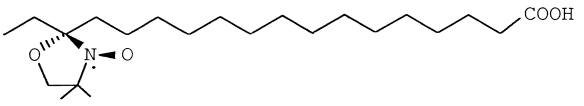

16-doxyl stearic acid (16-DXSA)

The nitroxides were purchased from Sigma, Munich, Germany, and used without further purification. A water solution of 10^{-2} mol/l of TEMPO and 10^{-2} mol/l ethanol solution of *n*-DXSA were prepared and diluted to 10^{-4} mol/l in the sample.

2.2. Preparation of cell suspensions from colon and breast tissues

Table 1 reports all information relevant to patients actually investigated, including age, sex, TNM staging, and the site of the lesion. The TNM classification system is based on anatomical extension of the tumor mass and is determined by clinical and histopathological measurements. The three components evaluated in the TNM classification are: T, extension

Table 1
Characteristics of the human colorectal tissues investigated in this work

Sample	Carcinoma	Adenoma	Sex	Age (years)	Lesion site	TNM	Liver metastasis
cr332		+	M	71	rectum	–	no
cr333	+		M	69	descending colon	T3N0	no
cr335	+		F	71	sigmoid colon	T3N0	no
cr339	+		F	58	sigmoid colon	T3N1	no
cr341	+		F	57	transverse colon	T3N0	no
cr343	+		F	72	sigmoid colon	T2N0	no
cr344	+		F	75	rectum	T3N0	no
cr501	+		M	70	transverse colon	T3N2a	yes
cr502	+		F	77	rectum	T3N0	no
cr503	+		F	83	ascending colon	T3N0	yes
cr504	+		F	82	ascending colon	T3N0	no
cr505	+		M	73	rectum	T3N1	yes

of the primary tumor mass; N, absence or presence and extension of metastasis in regional lymph nodes; and M, absence or presence of dislocated metastasis in other body regions [56].

In all tissues studied, parameters for prognosis prediction were measured, such as ^{3}H-thymidine labeling index (TLI), ploidy flow cytometry, and S-phase fraction (SPT). These cell kinetics parameters represent the proliferative activity of the tumor mass. They are now in elaboration for their biomedical aspects.

2.2.1. Materials used for the preparation of the cell suspensions

No frozen or fixed tissues were used. For the maintenance of the surgically removed tissues, McCoy's 5A powder culture medium was used. The final pH was 7.2–7.4. The McCoy's 5A culture medium contained antibiotics and the factors necessary for cell survival over a relatively long time. The composition of the medium is reported in Table 2.

2.2.2. Cell suspensions of human tissues

Cell suspensions to be analyzed by ESR were treated as it follows: (1) tissue breaking down by mechanical fragmentation; (2) filtration of the cell suspension with Nytex filter (pore diameter = 5×10^{-5} m); and (3) centrifugation (5 min at $350\times g$) and resuspension in the appropriate volume of McCoy's 5A medium. The count of the cell number was carried out with a Bürker hematocytometer. The largest fraction of cell suspensions contained mucosa cells and the smallest fraction ($\sim$10%) contained erythrocytes and lymphocytes.

2.3. ESR measurements

The samples to be analyzed were prepared with 990 μl of the cell suspension (containing cell concentration from 10^6 to 3×10^7 cell/ml) to which 10 μl of the suitable 10^{-2} mol/l nitroxide solution was added. The total nitroxide amount added in each sample was therefore 10^{-4} mol/l. The colorectal cells have a mean cell mass of 10^{-8} g and a lipid content in the range 5–10% w/w. On this basis the nitroxide/lipid molecular ratios were in the range 1:6 to 1:12 in the more diluted suspensions ($\sim10^6$ cell/ml) and in the range 1:200 to 1:400 in the more concentrated suspensions ($\sim3\times10^7$ cell/ml). These ratios are expected to not appreciably perturb cell membranes. This was proved by the analysis of the ESR lineshape (see following sections). After stirring for a few seconds at 310 K, 100 μl of the sample was inserted into quartz holder (i.d. 1 mm) and introduced into the ESR cavity of a Bruker ESR spectrometer model 200D operating at X-band ($\sim$9.5 GHz). All of the results reported in this work were obtained at physiological temperature (310 K). Temperature was controlled with the Bruker ST100–700 variable temperature assembly (accuracy $\pm$1 K). When kinetics data were collected, the time lag between sample preparation and the first spectrum was as shorter as possible. Typically this was 1–1.5 min.

The radical concentration was monitored from the

signal height as a function of time of the central peak in the first derivative ESR spectrum of the ^{14}N triplet in fast motion conditions (TAID, TEMPO adsorption intensity decay), as it has been previously established when the stability of the nitroxide into the cells is valued [18,40,44,46,49,51,57–63]. This required a careful control of the constancy of line shape and line width of the ESR absorption during the time of the experiment. The accuracy of this method was of the order of $\pm 5\%$. However, the major uncertainty in this kind of measurement was caused by the superposition of spectra arising from radicals in free motion and in slow motion domains (more hindered regions such as membranes) of the cell. The radicals in these two regions were in slow exchange in the ESR time scale and gave separate, overlapped absorptions. When this happened, the simple valuation of the signal height was no more a reliable parameter for radical concentration.

When the dynamics of the membrane was studied, single-cell suspensions were maintained in the culture medium and the appropriate amount of the nitroxide solution was added, in order to reach probe/cells ratio of $\leq 3\times 10^9$. The system was equilibrated for a few minutes at 310 K, then washed three times with Tris buffer and centrifuged in order to remove the unincorporate nitroxide molecules. Eventually, the centrifuged pellets were suspended again in 0.3 ml of the culture medium. The resulting suspension was analyzed by ESR.

The ESR magnetic parameters were obtained by using the calculation procedures reported by Schneider and Freed [64] and verified in most of the studies where the nitroxide dynamics is checked [65–73]. The main input parameters in this kind of calculation are: (a) the correlation time for the motion; this is usually (even if not always correctly) identified with the Debye–Stokes–Einstein reorienta-

Table 2
Composition of McCoy's 5A culture medium

Component	g/l ($\times 10^3$)	Component	g/l ($\times 10^3$)
L-alanine	13.36	L-ascorbic acid	0.50
L-arginine	42.14	biotin	0.20
L-asparagine•H_2O	45.03	D-calcium pantotenate	0.20
L-aspartic acid	19.97	choline hydrochloride	5.00
L-cysteine•HCl	31.53	folic acid	10.00
L-glutamic acid	22.07	inositol	36.00
L-glutamine	219.2	nicotinic acid	0.50
glutathione	0.50	nicotinamide	0.50
glycine	7.51	*p*-aminobenzoic acid	1.00
histidine•HCl•H_2O	20.96	piridossal•HCl	0.50
hydroxyproline	19.67	pyridossine•HCl	0.50
L-isoleucine	39.36	riboflavin	0.20
L-leucine	39.36	thiamine•HCl	0.20
L-lysine•HCl	36.54	vitamin B_{12}	2.00
L-methionine	14.92	$CaCl_2$•$2H_2O$	132.5
L-phenylalanine	16.52	KCl	400.0
L-proline	17.27	$MgSO_4$•$7H_2O$	200.0
L-serine	26.28	NaCl	6460
L-threonine	17.87	NaH_2PO_4•$2H_2O$	655.7
L-tryptophan	3.06	bactopeptone	600.0
L-tyrosine (disodium salt)	22.52	D-glucose	3000
L-valine	17.57	phenol red (sodium salt)	10.0
	IU/l		
penicillin G (sodium salt)	20,000		
dihydrostreptomycin sulfate	200.0		
gentamicin	16.00		

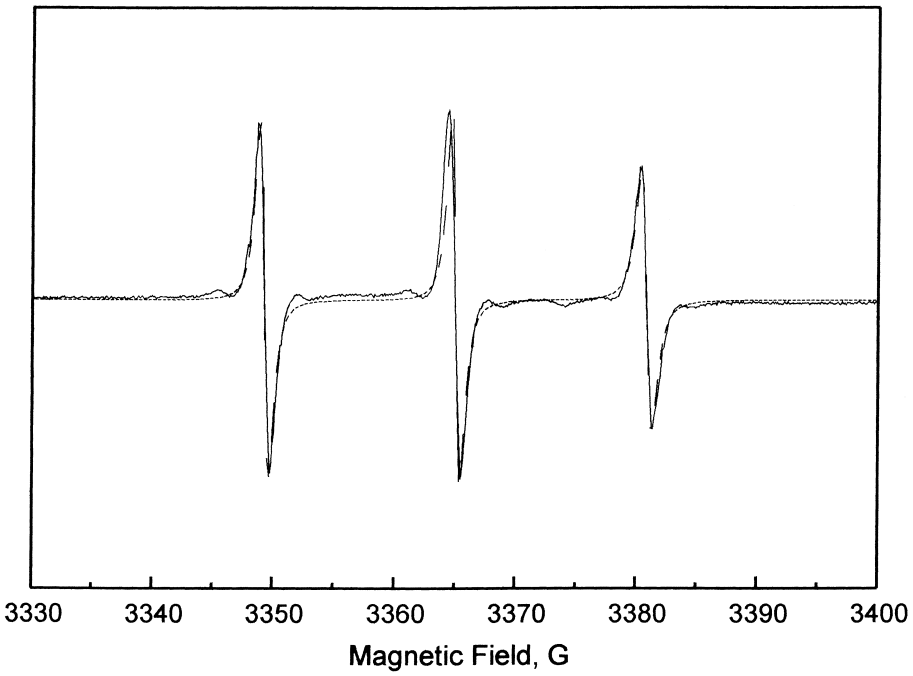

Fig. 1. ESR spectrum of 5-DXSA in McCoy's 5A culture medium: full line, experimental spectrum (T = 310 K); dashed line, calculated spectrum.

tional time of spherical objects, $\tau_c = 4\pi a^3 \eta / 3k_B T$, where a is the hydrodynamic radius of the reorienting object, η is the microviscosity, k_B the Boltzmann constant, and T the absolute temperature; (b) the components of the magnetic tensors $\boldsymbol{g}$ and $\boldsymbol{A}$, which may result in an anisotropic motion due to different diffusion coefficients; and (c) parameters which are related to the order of the environment in which the probe is inserted (the S_{33} index, as it results from the Saupe theory of the liquid crystals [74,75]). The accuracy of the parameters relevant for the motion has been reported in the text when appropriate.

3. Results

Although the McCoy's 5A culture medium contains small amounts of reducing agents, such as L-ascorbic acid and glutathione, all of the nitroxides used gave almost the same spectra in the culture medium and in 0.1 mol/l NH_4Cl water solution. No signal intensity decrease with time was observed in the culture medium. The spectra of TEMPO, 5- and 16-DXSA in McCoy's 5A culture medium were fitted with the same magnetic parameters as in NH_4Cl water solution (Table 3). Fig. 1 shows the

Table 3
Magnetic parameters used in the ESR spectrum simulation of 5-DXSA and 16-DXSA in McCoy's 5A culture medium at 310 K and in NH_4Cl water solution (0.1 M)

	g_{xx}	g_{yy}	g_{zz}	A_{xx} (G)	A_{yy} (G)	A_{zz} (G)	$T_{2,0}$ (G)	$<A>$ (G)	τ_c (s)
5-DXSA–water	2.0080	2.0062	2.0029	6.2	5.8	35.4	0.55	15.8	8×10^{-11}
16-DXSA–water	2.0080	2.0060	2.0029	6.2	5.8	35.4	0.6	15.8	5×10^{-11}
5-DXSA–McCoy's medium	2.008	2.0062	2.0029	6.2	5.8	35.4	0.5	15.8	1×10^{-10}
16-DXSA–McCoy's medium	2.008	2.0062	2.0029	6.2	5.8	35.4	0.55	15.8	6.5×10^{-11}

g_{xx}, g_{yy}, g_{zz}, and A_{xx}, A_{yy}, A_{zz} are the main components of the $\boldsymbol{g}$ tensor and of the hyperfine coupling $\boldsymbol{A}$ tensor; $T_{2,0}$ is the intrinsic linewidth due to non-motional effects; $<A>$ is the averaged hyperfine coupling constant (from: $<A> = (A_{xx}+A_{yy}+A_{zz})/3$); τ_c's are the mean correlation times used for the spectral simulations.

experimental ($T = 310$ K) ESR spectrum of 5-DXSA in McCoy's 5A culture medium and its shape calculated according to the Freed procedure with the best-fit magnetic parameters reported in Table 3.

Fig. 2 shows the variation with time of the height of the central line of TEMPO and *n*-DXSA radicals in healthy cells of colon (patient cr334, cell concentration 8×10^6 cell/ml; nitroxide/cell ratio = 8×10^9). TEMPO is a small, relatively water soluble molecule which is able to cross cell membranes. It localizes prevalently in extra- and intracellular aqueous environments. The ESR spectrum of TEMPO exhibited a fast motion character with a reorientation correlation time of the order of that found in pure water ($\tau_c = 5\times10^{-12}$ s; [76,77]). No overlap with slow motion spectra was observed during the experiment time. Thus, any apparent height decrease of the signal should be due to an actual nitroxide reduction to the diamagnetic hydroxylamine. However, the experimental points are affected by an error of ± 5%, and the signal intensity decrease should be considered as a small decrease of radical concentration.

The lipophilic nitroxides *n*-DXSA localize inside the membrane with the paramagnetic moiety exposed to different regions of the membrane itself. A very large fraction of the radical inserted into the membrane gave rise to slow motion spectra. This happened in the very first few minutes after the probe addition; then the slow motion/fast motion spectra ratio was practically invariant with time. Figs. 3 and 4 show the time dependence of the ESR spectra of 5- and 16-DXSA in neoplastic colon cells of the case cr504. Two points must be considered in the analysis of the spectra in Figs. 3 and 4. The first one is the intensities of the ESR absorptions, which were significantly lower (probably one order of magnitude) than expected from a 10^{-4} mol/l nitroxide solution. This was due to the fact that a large fraction of the added nitroxide underwent to reduction reaction when in contact with the enzyme system of the membrane. The second point is the relative intensities at different times reported as they appear in Fig. 4. It must be kept in mind that the reported spectra are obtained after different scanning as is explained in the caption to the figure. The ESR spectra in the healthy cells were not distinguishable from those of the transformed cells and are not reported. From spectral shape dependence on time, 5-DXSA incorporated more rapidly than 16-DXSA in the cell membranes. In any case, the use of cell suspension

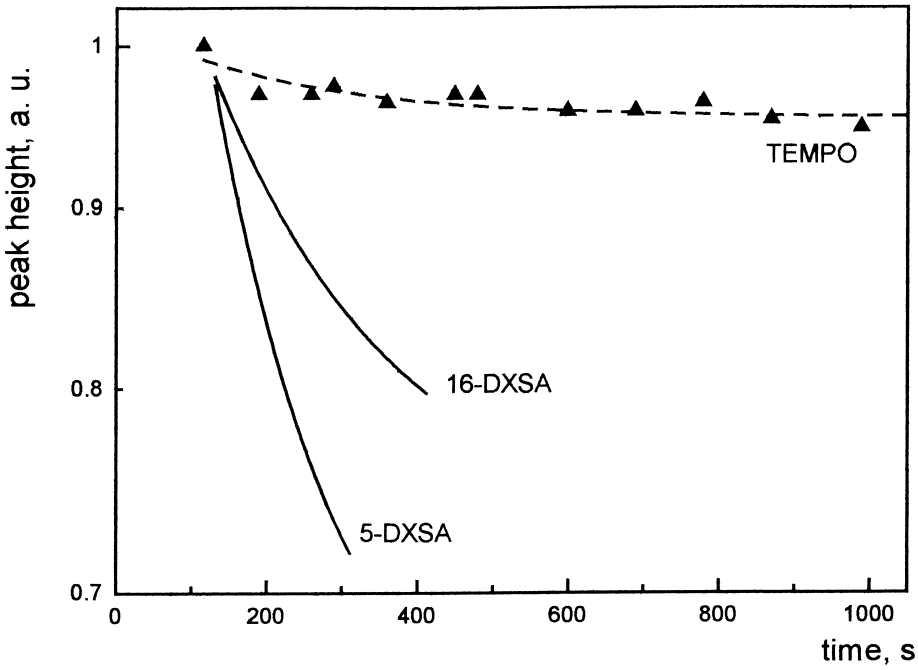

Fig. 2. Variation with time of the ESR central line peak height of TEMPO, 5- and 16-DXSA (cr334 healthy cells; cell concentration, 8×10^6 cell/ml; nitroxide/cell ratio, 8×10^9). For the DXSA nitroxides, only the trend of the peak height decrease is reported (see text for details).

with low nitroxide/cell ratios allowed us to assess that the rate of *n*-DXSA incorporation into the cell membrane was very rapid. The cell concentration was 10^7 cell/ml and the nitroxide/cell ratio was 6×10^9 to be compared with nitroxide/cell ratios $\geq10^{10}$ in the cases discussed above. Calculation of the spectral shape as a sum of fast- and slow-moving radical spectra indicated that peak height ratios comparable with those reported in the figures were obtained when the fast moving radical fraction was a few percent. The height decrease could therefore not be considered as a valuable tool for the study of the paramagnetism loss in colon cells containing lipophilic probes. This is particularly evident when the 5-DXSA spectrum height was considered. The signal height decreases shown in Fig. 2 for *n*-DXSA were therefore qualitative and they only represent a trend of the decrease of the central line of the fast moving spectrum due to rapid incorporation of the radicals into the membranes.

We must observe at this point that visible cell aggregates were formed because of sedimentation with time when suspensions containing relatively high cell

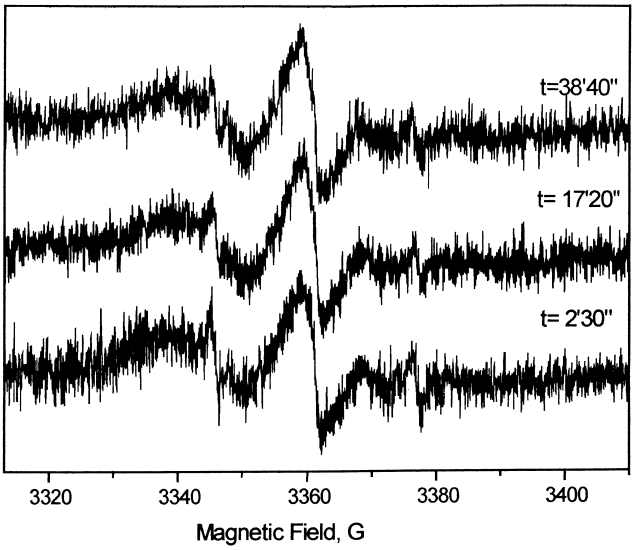

Fig. 3. 5-DXSA ESR spectra in tumor cells of the cr504 sample recorded 2 min 30 s, 17 min 20 s and 38 min 40 s after the addition of the lipophilic nitroxide to the cell suspension ($T=310$ K). Time values reported on each spectrum were taken at the middle point of the central line.

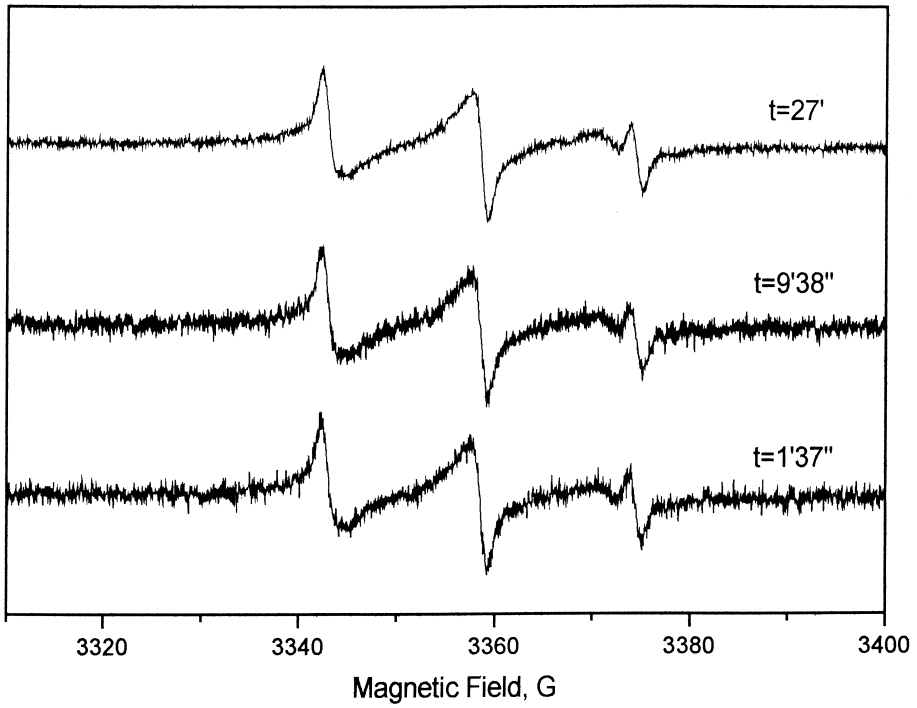

Fig. 4. 16-DXSA ESR spectra in tumor cells (cr504 sample) recorded at different times after the addition of the lipophilic nitroxide to the cell suspension. Spectra registered after 1 min 37 s and 9 min 38 s were scanned only once, whereas the spectrum after 27 min was scanned five times. This justifies the increased signal-to-noise ratio with respect to the other spectra.

Table 4
Magnetic parameters used in the ESR simulation of 5-DXSA spectrum in three different cases of healthy and neoplastic colorectal human tissues

	g_{xx}	g_{yy}	g_{zz}	A_{xx} (G)	A_{yy} (G)	A_{zz} (G)	$\tau_{\|}$ (s)	$\tau_{\perp}$ (s)	n	λ	$<g>$	$<A>$ (G)	τ_c (s)	S_{33}
Cr343														
Health	2.0083	2.0070	2.0029	5.00	5.00	32.8	6.3×10^{-10}	6.3×10^{-9}	10	2.0	2.0061	14.3	$2\cong\times10^{-9}$	0.44
Tumor	2.0083	2.0070	2.0029	5.00	5.00	32.8	6.3×10^{-10}	6.3×10^{-9}	10	2.0	2.0061	14.3	2×10^{-9}	0.44
Cr341														
Health	2.0083	2.0070	2.0029	5.00	5.00	32.8	7.4×10^{-10}	7.4×10^{-9}	10	1.8	2.0061	14.3	1.8×10^{-9}	0.39
Tumor	2.0083	2.0070	2.0029	5.00	5.00	32.8	7.4×10^{-10}	7.4×10^{-9}	10	1.8	2.0061	14.3	1.8×10^{-9}	0.39
Cr344														
Health	2.0083	2.0070	2.0029	5.00	5.00	32.8	8×10^{-10}	8×10^{-9}	10	2.0	2.0061	14.3	2.5×10^{-9}	0.44
Tumor	2.0083	2.0070	2.0029	5.00	5.00	32.8	6.12×10^{-10}	6.12×10^{-9}	10	1.8	2.0061	14.3	1.5×10^{-9}	0.39

Accuracy: $\Delta A_{zz}=\pm1$ G; $\Delta A_{yy}=\Delta A_{xx}=0.5$ G, $\Delta n=\pm2$; $\Delta\lambda=\pm0.3$,$\Delta<g>=\pm0.0005$; $\Delta<A>=\pm0.6$ G; $\Delta\tau_c=\pm0.3\times10^{-9}$ s.; $\Delta S=\pm0.07$. For the definition of g_{ii}, A_{ii}, $<g>$, $<A>$, τ_c see Table 3. $\tau_{\|}$ and $\tau_{\perp}$ represent the reorientation times along the longer and the shorter axes of the nitroxide molecules, respectively; n is the anisotropy parameter, $n=\tau_{\perp}/\tau_{\|}$; λ is a coefficient related to the order parameter [64]; S_{33} is the order parameter arising from spectral simulations.

Fig. 5. 5-DXSA ESR spectra in healthy cell suspension of cr343 sample: full line, experimental shape ($T=310$ K); dashed line, calculated shape. Cell concentration $=2.7\times10^7$ cell/ml; [5-DXSA] $=10^{-4}$ M; nitroxide/cell $=2.2\times10^9$.

number were prepared. Samples prepared in controlled, reproducible conditions were therefore always analyzed. A complete elimination of the free component in the system whose spectrum was registered was achieved with difficulty either by changing the nitroxide/cell ratio or by repeated washing of the samples. When a correct nitroxide/cell ratio was found, a trial and error procedure of subtraction of the fast motion component from the experimental absorption was carried out. The typical spectrum of slow moving DXSA was obtained as is shown for 5-DXSA in the Fig. 5 (cr343, healthy cells, cell content in the suspension 2.7×10^7/ml; nitroxide/cell ratio $=2.2\times10^9$). This spectrum did not substantially differ from the 5-DXSA spectrum in malignant cell of the same patient. This procedure was also followed with 16-DXSA, which was in agreement with above observations on 5-DXSA.

Table 4 reports correlation times for the motion of the 5-DXSA probe along the long molecular axis ($\tau_{\|}$) and along the normal to this axis ($\tau_{\perp}$), their mean values, the calculated order parameter S_{33}, together with the anisotropic components of the $\boldsymbol{g}$ and $\boldsymbol{A}$ tensors which gave the best fit with the experimental spectra in healthy and neoplastic cells from patients with a different history. The mean correlation times

of the probe were in the range $1.8–2.5\times10^{-10}$ s with a significant motional anisotropy ($n=\tau_{\perp}/\tau_{||}=10$). The $\boldsymbol{g}$ and $\boldsymbol{A}$ components were the same in all the calculated samples. With 16-DXSA used as spin label, the best fit parameters obtained from the simulation of the spectra did not show any difference from healthy and neoplastic tissues.

4. Discussion

The ESR results reported in this paper were obtained from healthy and neoplastic cells of colon, that were kept in a living state after surgery in a McCoy's 5A culture medium.

As a first observation, we must note that no free radicals were detected as originated from the neoplastic process, which meant that free radicals produced by tumor formation or responsible for its formation, if they existed, had life times too short to be detected during a typical ESR experiment.

A few cases have been reported of relatively stable radicals which have been correlated with the cancer development. In healthy and neoplastic tissues of human liver, a comparison has been made between the intensity of a $g\sim2$ signal, which was at least ten times stronger in the structural parts of the healthy cells than in tumor cells [4]. No differences are found in the soluble fractions of normal and tumor tissues. The $g\sim2$ signal intensity change has also been the main criterion used by Swartz and coworkers [5,78] in their studies on cells of rat Walker 256 carcinosarcoma. Unfortunately, the line shape does not allow a correct identification of the radicals responsible for the absorptions and no clear mention is made that normal and transformed tissues of the same patient or animal are used. At the same time, the features of the ESR spectra arising from radicals claimed as responsible for the effects of α-tocopherol succinate on melanoma B16 cells are discussed.

We were interested in the stability of nitroxides into malignant tissues and from this point of view the analysis of the results has some interesting features regarding both the paramagnetism loss due to probe reduction (metabolism) and the mobility of probes inserted in different kinds of membranes.

The first effect has been widely investigated in non-living systems, such as cell fractions, membranes, etc. and it has been very often found that nitroxides are reduced with a rate dependent on system, temperature, and/or nitroxide structure, in the sense that five-membered nitroxides are more resistant to reduction than six-membered nitroxides [16,46,54,79]. This has been recently demonstrated in our laboratory in proliferating *Bacillus subtilis* cultures, where doxyl nitroxides appear to be the most susceptible towards reductions [62]. This fact should be kept in mind when new reduction-resistant nitroxide-based NMR contrast agents are designed or used in ESR imaging. The latter technique has indeed been used to allow 3D spatial as well as spectral-spatial imaging of two, three, or four dimensions at L-band of the distribution of nitroxides in isolated rat heart [26, 50,80].

Nitroxide stable free radicals have demonstrated properties favoring their use as NMR contrast media. Preliminary studies using a piperidinyl-oxyl radical as a NMR contrast medium for study of the kidney were reported more than 15 years ago by Brasch et al. [26]. The radical is rapidly excreted in the urine and its transient accumulation in renal structures notably increases NMR intensity. The same authors have employed *N*-succinyl derivative of 4-amine-TEMPO. Particular attention is given to the excretion of the radical: 60% of the total nitroxide administered dose was recovered in the urine by measuring the ESR signal indicating some in vivo metabolism, the remaining being reduced to hydroxylamine. No adverse effects, such as convulsions or death, were observed in the experimental animals. The rate of reduction is found to depend on the physiological and pathological conditions, such as aging, oxidative stress, hypoxia, hyperoxia, etc.

In both healthy and malignant colorectal tissues investigated in this paper no appreciable paramagnetism loss occurred even after long time exposure of tissues to small, water-soluble nitroxides. The reduction rate has been used in the past in cancer research. Voest et al. [63] report on the ESR signal decay of TEMPO in tumoral breast cells (MCF-7) and in pre-myelocytic leukemia cells (ML-60) treated with doxorubicin, which is suggested to mediate the cellular production of superoxide ions. The in vivo and in vitro nitroxide bioreduction in B16 melanoma decreases about 40% as a consequence of hypothermia [18]. Hypoxia and normoxia also change the re-

dox state of B16 melanoma [81]. Although the use of nitroxides to follow changes of redox potential in human organs is particularly attractive, it would therefore require more subtle forms of molecular control in the context of colorectal cancer. For instance, the observed stability of nitroxides at high concentration in mucosa cells could help to resolve the image of mucosa cells lining from other tissues. This task is, however, well beyond the aim of the present work.

When hydrophobic DXSA radicals were used, a partition equilibrium of the nitroxide between free and restricted motional domains was established in a few minutes and the mean isotropic contact constant $< A_N >$, as calculated from $A_{||}$ and $A_{\perp}$ values used for spectral fitting, decreased from 15.3 G in McCoy's 5A medium to 14.3 G hydrophobic cell membranes as expected for radical sensing less polar environments. Thus, an exact comparison of the total intensity variation with time of the absorption with that of the starting signal was not reliable because of the different shapes. However, a simple integration of the absorptions did not reveal large intensity changes with time. Calculation proves that when a few % of the fast motion signal overlaps to that of the slowly motion signal, the observed line shape is dominated by the fast signal in a more marked way than in the ESR spectra discussed in this paper. The largest fraction of *n*-DXSA, which was evaluated to be $>95\%$, was therefore embedded into double layers of the membranes. Apart from the time lag immediately after addition of the radical, the observed partition did not depend on time. Also in the case of hydrophobic nitroxides, the resistance of colon cells to the weak oxidant action of nitroxides seemed therefore high enough to suggest these compounds as stable MRI contrast agents for colorectal tumor.

The ESR spectra of nitroxides inserted into membranes offer a good alternative to the analysis of cell metabolism of the same compounds when relevant features of the membranes, such as mobility, polarity, order degree, in healthy and transformed cells are compared. Sentjurc et al. [82] give a series of results obtained from the methyl ester of 5-doxylpalmitate in different histotypes of brain tumors whose changes in fluidity during chemotherapy is addressed. In rat muscle and liver and in tumoral human brain, the authors found a probe fluidity lower in malignant cells than in normal cells. The effect of chemotherapy drugs is also investigated. The same procedure of spectral analysis is followed by Gaffney [15] on fibroblasts of mice embryos as compared to the same cells transformed by DNA and RNA virus and by methylcolanthrene.

In our samples, the 5-DXSA spectra were the more informative spectra on the molecular motions inside membranes. Slightly anisotropic correlation times of the order $2–3\times10^{-9}$ s fitted the experimental spectra indicating a relatively high membrane fluidity with appreciable order parameters (Table 4). For the same patient, the same spectra were registered at 310 K in both healthy and neoplastic cells. This meant that the incipient neoplasia did not alter mechanical properties of colorectal cell membrane system. Significant differences were observed when data from patients with different clinical history were compared (see, for instance, patient cr344, in which a large number of red blood cells was detected in the tumor cells, with resultant lower $< \tau_c >$ values; see Table 4).

The same considerations applied when 16-DXDA spectra were analyzed. In fact, when 16-DXSA was used as a spin label, the membrane region probed by the spin label was the inner, more mobile region. The best fit parameters obtained from the simulation of these spectra did not show any difference in either line shape or mobility between normal and cancer cells.

The analysis of the nitroxide dynamics into healthy and malignant cells gives insight on important effects of candidate contrast agents on phospholipid membranes. Furthermore, their ability to cross the cellular membranes or to be inserted in them is one of the most speculated aspects of the contrast-enhancing agents [83,84].

When the results reported in this paper are judged, it is necessary to consider that the systems are very complex and an unambiguous structural model that may describe them is difficult to build. A cell suspension comprises living epithelial cells together with other kinds of cell with differently structured membranes, and extracellular elements, such as membrane fragments, organelles, etc. Spectral simulations better than those shown here could surely be performed, but the improvement of the magnetic param-

eters for a better fitting was largely of the order of the experimental errors.

Acknowledgements

Thanks are due to Italian Ministero della Università e della Ricerca Scientifica (MURST) and to Consiglio Nazionale delle Ricerche (CNR) for funding this research. Thanks are also due to Prof. C. Cortesini and to Dr. F. Cianchi of Clinica Chirurgica Generale, University of Florence, for the tissues we used in this work.

References

[1] P.G. Morris, Nuclear Magnetic Resonance Imaging in Medicine and Biology, Clarendon Press, Oxford, 1986.
[2] H.M. Swartz, in: G. Klein, S. Weinhouse (Eds.), Advances in Cancer Research, Academic Press, New York, 1972, pp. 227–252.
[3] H.M. Swartz, in: D. Armstrong, R. Sohal, R. Cutler, T. Slater (Eds.), Free Radicals in Molecular Biology and Aging, Raven Press, New York, 1984, pp. 275–292.
[4] F.E. Knock, P.R.C. Gascoyne, Physiol. Chem. Phys. 13 (1981) 447–454.
[5] H.M. Swartz, P.L. Gutierrez, Science 198 (1977) 936–938.
[6] P. Ottino, J.R. Duncan, Free Radic. Biol. Med. 22 (1997) 1145–1151.
[7] P. Ottino, J.R. Duncan, Nutr. Res. 17 (1997) 661–676.
[8] M. Miyake, S. Fushimoto, H. Iwagaki, N. Matsubara, R. Edamatsu, M. Hiramatsu, K. Orita, Res. Commun. Chem. Pathol. Pharmacol. 71 (1991) 293–307.
[9] N. Matsubara, M. Hiramatsu, R. Edamatsu, K. Mizukawa, A. Mori, K. Orita, Free Radic. Biol. Med. 22 (1997) 679–687.
[10] Y. Nonaka, H. Iwakaki, T. Kimura, S. Fushimoto, K. Orita, Int. J. Cancer 54 (1993) 983–986.
[11] H.J. Halpern, C. Yu, E.D. Barth, M. Peric, G.M. Rosen, Proc. Natl. Acad. Sci. USA 92 (1995) 796–800.
[12] H.J. Halpern, C. Yu, M. Peric, E.D. Barth, G.S. Karczmar, J.N. River, D.J. Grolina, B.A. Teicher, Radiat. Res. 145 (1996) 610–618.
[13] P.M. Plonka, B.K. Plonka, S. Pajak, S.J. Lukiewicz, Curr. Top. Biophys. 20 (1996) 46–52.
[14] C. Benedetto, A. Bocci, M.U. Dianziani, Cancer Res. 41 (1981) 2936–2942.
[15] B. Gaffney, Proc. Natl. Acad. Sci. USA 72 (1975) 664–668.
[16] M. Sentjurc, S. Pecar, K. Chen, M. Wu, H.M. Swartz, Biochim. Biophys. Acta 1073 (1991) 329–335.
[17] E.E. Voest, E. van Fassen, B.S. van Asbeck, J.P. Neijt, J.J.M. Marx, Biochim. Biophys. Acta 1136 (1992) 113–118.
[18] M. Elas, M.K. Cieszka, Z. Matuszak, S. Lukiewicz, Curr. Top. Biophys. 20 (1996) 62–66.
[19] D. Gelvan, P. Saltman, R.S. Powell, Proc. Natl. Acad. Sci. USA 88 (1991) 4680–4684.
[20] M.C. Krishna, A. Russo, J.B. Mitchell, S. Goldstein, H. Dafni, A. Samuni, J. Biol. Chem. 271 (1996) 26026–26031.
[21] A. Samuni, C. Murali-Krishna, P. Riesz, A. Finkelstein, A. Russo, J. Biol. Chem. 34 (1988) 17921–17924.
[22] J.B. Mitchell, A. Samuni, M.C. Krishna, W.G. DeGraff, M.S. Ahn, U. Samuni, A. Russo, Biochemistry 29 (1990) 2802–2807.
[23] J.B. Mitchell, W. DeGraff, D. Kaufman, M.C. Krishna, A. Samuni, E. Finkelstein, M.S. Ahn, J. Gamson, A. Russo, Arch. Biochem. Biophys. 289 (1991) 62–70.
[24] G.Y. Wang, D. Godinger, J. Aranovitch, A. Samuni, Biochim. Biophys. Acta 1305 (1996) 71–78.
[25] B. Gallez, R. Demeure, R. Debuyst, D. Leonard, F. Dejehet, P. Dumont, Magn. Reson. Imag. 10 (1992) 445–455.
[26] R.C. Brasch, D.A. London, G.E. Wesbey, T.N. Tozer, D.E. Nitecki, R.D. Williams, J. Doemeny, L. Dallas Tuck, D.P. Lallemand, Radiology 147 (1983) 773–779.
[27] B. Gallez, V. Lacour, R. Demeure, R. Debuyst, F. Dejehet, J.L. De Keyser, P. Dumont, Magn. Reson. Imag. 12 (1994) 61–69.
[28] F. Goda, B. Gallez, H.M. Swartz, Res. Chem. Interm. 22 (1996) 491–498.
[29] H.F. Bennett, R.D. Brown III, J.F.W. Keana, S.H. Koenig, H.M. Swartz, Magn. Reson. Med. 14 (1990) 40–55.
[30] H.M. Swartz, in: E. Feig (Ed.), Advances in Magnetic Resonance Imaging, Ablex, Norwood, 1989, p. 49.
[31] P.C. Lauterbur, M.H. Mendonca-Dias, A.M. Raudin, Front. Biol. Eng. 1 (1978) 752–759.
[32] F. Bloch, W.W. Hansen, M. Packard, Phys. Rev. 70 (1946) 474–485.
[33] W. Schörner, R. Felix, M. Laniado, L. Lange, H.J. Weinmann, C. Claussen, W. Fiegler, U. Speck, E. Katzner, ROFO 140 (1984) 493–500.
[34] T. Fritsch, W.W. Krause, H.J. Weinmann, J. Eur. Radiol. 2 (1992) 2–13.
[35] E.G. Ankel, C.-S. Lai, L.E. Hopwood, Z. Zivkovic, Life Sci. 40 (1987) 495–498.
[36] V. Afzal, R.C. Brasch, D.E. Nitecki, S. Wolff, Invest. Radiol. 19 (1984) 549–552.
[37] E.J. Rauckman, G.M. Rosen, L.K. Griffeth, in: Spin Labeling in Pharmacology, Academic Press, New York, 1989, pp. 175–190.
[38] S. Belkin, R.J. Mehlhorn, K. Hideg, O. Hankowsky, Arch. Biochem. Biophys. 26 (1987) 232–243.
[39] P.D. Morse II, H.M. Swartz, Magn. Reson. Med. 2 (1985) 114–127.
[40] L.K. Griffeth, G.M. Rosen, E.J. Rauckman, B.P. Drayer, Invest. Radiol. 19 (1984) 553–562.
[41] A.D. Keith, A.S. Waggoner, O.H. Griffith, Proc. Natl. Acad. Sci. USA 61 (1968) 819–826.
[42] A.D. Keith, G. Bulfield, W. Snipes, Biophys. J. 10 (1970) 618–629.

[43] A.T. Quintanilha, L. Packer, Proc. Natl. Acad. Sci. USA 74 (1977) 570–574.
[44] K. Chen, H.M. Swartz, Biochim. Biophys. Acta 970 (1988) 270–277.
[45] M. Kveder, M. Santjurc, M. Schara, Magn. Reson. Med. 8 (1988) 241–247.
[46] A. Iannone, A. Tomasi, V. Vannini, H.M. Swartz, Biochim. Biophys. Acta 1034 (1990) 290–293.
[47] V. Quaresima, C.L. Ursini, G. Gualtieri, A. Sotgiu, M. Ferrari, Biochim. Biophys. Acta 1182 (1993) 115–118.
[48] J. Fuchs, N. Groth, T. Herrling, G. Zimmer, Free Radic. Biol. Med. 22 (1997) 967–976.
[49] M. Branca, T. Denurra, F. Turrini, Free Radic. Biol. Med. 5 (1988) 7–11.
[50] J.L. Zweier, M. Chzhan, P.-G. Wang, P. Kuppusami, Res. Chem. Intermed. 22 (1996) 615–624.
[51] W.R. Couet, R.C. Brasch, G. Sosnowsky, J. Lukszo, I. Prakash, G.T. Gnewuch, T.N. Tozer, Tetrahedron 41 (1985) 1165–1172.
[52] J.F.K. Keana, F.L. Van Nice, Physiol. Chem. Phys. Med. NMR 16 (1984) 477–480.
[53] J.F.K. Keana, S. Pou, Physiol. Chem. Phys. Med. NMR 17 (1985) 235–240.
[54] J.F.K. Keana, S. Pou, G.M. Rosen, Magn. Reson. Med. 5 (1987) 525–536.
[55] P. Vallet, Y. Van Haverbeke, P.A. Bonnet, G. Subra, J.-P. Chapat, R.N. Muller, Magn. Reson. Med. 32 (1994) 11–15.
[56] L.H. Sobim, Ch. Wittekind (Eds.), UICC, TNM Classification of Malignant Tumors, Wiley-Liss, New York, 1997.
[57] C. Ebel, K.U. Ingold, J. Michon, A. Rassat, Tetrahedron Lett. 26 (1985) 741–744.
[58] Y. Kotake, Z. Yu, E.G. Janzen, Redox Rep. 2 (1996) 133–139.
[59] P. Kuppusami, P.H. Wang, J.L. Zweier, Magn. Reson. Chem. 33 (1995) S123–S128.
[60] M. Kveder, G. Pifat, S. Pecar, M. Schara, P. Ramos, H. Esterbauer, Chem. Phys. Lipids 85 (1997) 1–12.
[61] S. Morris, G. Sosnovsky, B. Hui, C.O. Huber, N.U.M. Rao, H.M. Swartz, J. Pharm. Sci. 80 (1990) 149–152.
[62] K. Jung, S. Ristori, E. Gallori, G. Martini, Biochim. Biophys. Acta 1425 (1998) 387–397.
[63] E.E. Voest, E. van Fassen, J.J.M. Marx, Free Radic. Biol. Med. 15 (1993) 589–595.
[64] D.J. Schneider, J.H. Freed, in: L.J. Berliner, J. Reuben (Eds.), Biological Magnetic Resonance, Vol. 8, Spin Labeling. Theory and Applications, Plenum Press, New York, 1989, p. 1.
[65] J.J. Volwerk, O.H. Griffith, Magn. Reson. Rev. 13 (1988) 135–178.
[66] D. Marsh, in: L.J. Berliner, J. Reuben (Eds.), Biological Magnetic Resonance, Vol. 8, Spin Labeling. Theory and Applications, Plenum Press, New York, 1989, pp. 255–303.
[67] D. Marsh, in: G. Pifat-Mrzljak (Ed.), Supramolecular Structure and Function, Springer Verlag, Berlin, 1986, p. 48.
[68] Seelig, in: L.J. Berliner (Ed.), Spin Labeling. Theory and Applications, Vol. 1, Academic Press, New York, 1976, p. 373.
[69] O.H. Griffith, in: L.J. Berliner (Ed.), Spin Labeling. Theory and Applications, Vol. 1, Academic Press, New York, p. 454.
[70] D.A. Butterfield, in: L.J. Berliner, J. Reuben (Eds.), Biological Magnetic Resonance, Vol. 4, Plenum Press, New York, 1982, p. 1.
[71] N.J.F. Dodd, in: M.A. Foster (Ed.), Magnetic Resonance in Medicine and Biology, Pergamon Press, Oxford, 1984, pp. 66–91.
[72] M. Hemminga, Chem. Phys. Lipids 32 (1983) 323–383.
[73] N. Koercherginski, H.M. Swartz (Eds.), Nitroxide Spin Labels, CRC Press, Boca Raton, FL, 1995.
[74] A. Saupe, Z. Naturforsch. 19a (1964) 161–171.
[75] A. Saupe, Angew. Chem. 80 (1968) 99–115.
[76] S. Ristori, C. Maggiulli, J. Appell, G. Marchionni, G. Martini, J. Phys. Chem. B 101 (1997) 4155–4165.
[77] S. Ristori, S. Rossi, G. Ricciardi, G. Martini, J. Phys. Chem. B 101 (1997) 8507–8512.
[78] P.L. Gutierrez, H.M. Swartz, E.J. Wilkinson, Br. J. Cancer 39 (1979) 330–336.
[79] W.R. Couet, R.C. Brasch, G. Sosnowsky, T.N. Tozer, Magn. Reson. Imaging 3 (1985) 83–88.
[80] H. Utsumi, K. Takeshita, in: H. Ohya, L. Packer (Eds.), Bioradicals Detected by ESR Spectroscopy, Birkäuser, Basel, 1992, pp. 321–334.
[81] K. Cieszka, M. Elas, Z. Matuszak, S. Lukiewicz, Curr. Top. Biophys. 20 (1996) 58–61.
[82] M. Sentjurc, M. Schara, M. Auersperg, M. Jezernik, M. Kveder, Studia Biophys. 136 (1990) 201–208.
[83] H.-J. Weinmann, H. Bauer, T. Frenzel, H. Gries, H. Schmitt-Willich, G. Shumann-Giamperi, H. Vogler, Contrast Enhanced Magnetic Resonance: Workshop Syllabus, 1991, Napa, CA, May 23–25.
[84] T. Smirnova, A.I. Smirnov, R.L. Belford, R.B. Clarkson, J. Am. Chem. Soc. 120 (1998) 5060–5072.